

This is a repository copy of *Photovoltaic fault detection algorithm based on theoretical curves modelling and fuzzy classification system*.

White Rose Research Online URL for this paper:

<https://eprints.whiterose.ac.uk/177678/>

Version: Accepted Version

---

**Article:**

Dhimish, Mahmoud, Holmes, Violeta, Mehrdadi, Bruce et al. (2 more authors) (2017) Photovoltaic fault detection algorithm based on theoretical curves modelling and fuzzy classification system. *Energy*. pp. 276-290. ISSN 0360-5442

<https://doi.org/10.1016/j.energy.2017.08.102>

---

**Reuse**

Items deposited in White Rose Research Online are protected by copyright, with all rights reserved unless indicated otherwise. They may be downloaded and/or printed for private study, or other acts as permitted by national copyright laws. The publisher or other rights holders may allow further reproduction and re-use of the full text version. This is indicated by the licence information on the White Rose Research Online record for the item.

**Takedown**

If you consider content in White Rose Research Online to be in breach of UK law, please notify us by emailing [eprints@whiterose.ac.uk](mailto:eprints@whiterose.ac.uk) including the URL of the record and the reason for the withdrawal request.

# Photovoltaic Fault Detection Algorithm Based on Theoretical Curves Modelling and Fuzzy Classification System

Mahmoud Dhimish, Violeta Holmes, Bruce Mehrdadi, Mark Dales, Peter Mather

Department of Computing and Engineering, University of Huddersfield, Huddersfield, United Kingdom

---

## *Abstract*

This work proposes a fault detection algorithm based on the analysis of the theoretical curves which describe the behaviour of an existing PV system. For a given set of working conditions, solar irradiance and PV modules' temperature, a number of attributes such as voltage ratio (VR) and power ratio (PR) are simulated using virtual instrumentation (VI) LabVIEW software. Furthermore, a third order polynomial function is used to generate two detection limits for the VR and PR ratios obtained using VI LabVIEW simulation tool.

The high and low detection limits are compared with measured data taken from 1.1kWp PV system installed at the University of Huddersfield, United Kingdom. Samples lie out of the detection limits are processed by a fuzzy logic classification system which consists of two inputs and one output membership function.

In this paper, PV faults corresponds to a short circuited PV module. The obtained results show that the fault detection algorithm can accurately detect different faults occurring in the PV system, where the maximum detection accuracy of before considering the fuzzy logic system is equal to 95.27%. However, the fault detection accuracy is increased up to a minimum value of 98.8% after considering the fuzzy system.

**Keywords:** *Photovoltaic Faults, Fault Detection, Fuzzy Logic, PV Hot Spot Detection, LabVIEW.*

---

## *1. INTRODUCTION*

Despite the fact that Grid-Connected Photo-Voltaic (GCPV) systems have no moving parts, and therefore usually require low maintenance, they are still subject to various failures and faults associated with the PV arrays, batteries, power conditioning units, utility interconnections and wiring [1 and 2]. It is especially difficult to shut down PV modules completely during faulty conditions related to PV arrays (DC side) [3]. It is therefore required to create algorithms to facilitate the detection of possible faults occurring in GCPV systems [4].

There are existing fault detection techniques for use in GCPV plants. Some use satellite data for fault prediction as presented by M. Tadj et al [5], this approach is based on satellite image for estimating solar radiation data and predicting faults occurring in the DC side of the GCPV plant. However, some algorithms do not require any climate data, such as solar irradiance and modules' temperature, but instead use earth capacitance measurements in a technique established by Taka-Shima et al [6].

38 Some fault detection methods use an automatic supervision based on the analysis of the output power for  
39 the GCPV system. A. Chouder & S. Silvestre et al [7], presented a new automatic supervision and fault  
40 detection technique which use a standard deviation method ( $\pm 2\sigma$ ) for detecting various faults in PV  
41 systems such as faulty modules in a PV string and faulty maximum power point tracking (MPPT) units.  
42 However, S. Silvestre et al [8] presented a new fault detection algorithm based on the evaluation of the  
43 current and output voltage indicators for analyzing the type of fault occurred in PV systems installations.

44 A photovoltaic fault detection technique based on artificial neural network (ANN) is proposed by W.  
45 Chine et al [9]. The technique is based on the analysis of the voltage, power and the number of peaks in  
46 the current-voltage (I-V) curve characteristics. However, [10 and 11], proposed a fault detection algorithm  
47 which allows the detection of seven different fault modes on the DC-side of the GCPV system. The  
48 algorithm uses the t-test statistical analysis technique for identifying the presence of systems fault  
49 conditions.

50 Other fault detection algorithms focus on faults occurring on the DC and AC-side of PV systems, as  
51 proposed by M. Dhimish et al [12]. The approach uses T-test statistical analysis technique for identifying  
52 the faulty conditions in the DC/AC inverter and MPPT units. Moreover, hot-spot detection in PV  
53 substrings using the AC parameters characterization was developed by [13]. The hot-spot detection  
54 method can be further used and integrated with DC/DC power converters that operates at the subpanel  
55 level. Nevertheless, the hot spot mitigation due to the impact of micro cracks is described in [14].

56 A comprehensive review of the faults, trends and challenges of the grid-connected PV systems is  
57 explained by M. Obi & R. Bass, M. Alam et al and A. khamis et al [15-17].

58 Currently, fuzzy logic systems widely used with GCPV plants. R. Boukenoui et al [18] proposed a new  
59 intelligent MPPT method for standalone PV system operating under fast transient variations based on  
60 fuzzy logic controller (FLC) with scanning and storing algorithm. Furthermore, [19] presents an adaptive  
61 FLC design technique for PV inverters using differential search algorithm.

62 B. Abdesslam et al [20] proposed a neuro-fuzzy classifier for fault detection and classification in PV  
63 systems, the approach is suitable for detection faulty conditions such as detected bypass diodes and  
64 blocking diodes faults. Furthermore, [21] proposed a cascaded fuzzy logic based arc fault detection in PV  
65 modules using an analog-digital converter (ADC) contained in micro controllers.

66 Since many fault detection algorithms use statistical analysis techniques such as [7, 10, 11 and 12], this  
67 work proposes a fault detection algorithm that does not depend on any statistical approaches in order to  
68 classify faulty conditions in PV systems. Furthermore, some existing fault detection techniques such as  
69 [22 and 23] use a complex power circuit design to facilitate the fault detection in GCPV plants. However,  
70 the proposed fault detection algorithm depends only on the variations of the voltage and the power, which  
71 makes the algorithm simple to construct and reused in wide range of GCPV plants.

72 In this paper, the PV fault corresponds to short circuited PV module in PV strings. The short circuit PV  
73 detection techniques have been also developed by many researchers. In [24] authors have proposed a  
74 smart algorithm based on support vector machine (SVM) technique for diagnosis short circuit faults in PV  
75 systems. Another technique based on semi-supervised learning for PV fault detection and classification is  
76 presented by [25].

77 On the other hand, the short circuit faults in PV systems can be detected using a decision tree-based fault  
78 classification method as proposed in Y. Zhao et al [26]. In addition, the open and short circuit switch  
79 failure in the PV systems DC/DC converters can be detected using the time and PV current criteria which

80 observe the slope of the inductor current over the time [27]. Moreover, the performance of PV modules  
81 under open and short circuit faults has been modelled and classified using simulation analysis of the PV I-  
82 V curves was developed by [28].

83 Generally, in order to examine PV plants, it is always recommended to have a suitable PV monitoring and  
84 logging units. LabVIEW software has been used by many researchers to monitor, model and analyze the  
85 performance of the PV plants [29-33]. In [29-30], LabVIEW software has been used to model and  
86 simulate the theoretical performance of a PV systems. However, in [31] authors have used LabVIEW to  
87 examine the dynamic and transient characteristics of PV systems. Most recently, LabVIEW software has  
88 been used to monitor and enhance the dynamic modelling of the PV battery storage as proposed by [32].  
89 Furthermore, the classification of PV faults using t-test statistical method using LabVIEW simulation is  
90 developed by M. Dhimish et al [33].

91 In this work, we present the development of a fault detection algorithm which allows the detection of  
92 possible faults occurring on the DC-side of GCPV systems. The algorithm is based on the analysis of  
93 theoretical voltage ratio (VR) and power ratio (PR) for the examined GCPV system. High and low  
94 detection limits are generated using 3<sup>rd</sup> order polynomial functions which are obtained using the simulated  
95 data of the VR and PR ratios. Subsequently, if the theoretical curves are not capable to detect the type of  
96 the fault occurred in the GCPV system, a fuzzy logic classifier system is designed to facilitate the fault  
97 type detecting for the examined PV system.

98 A software tool is designed using Virtual Instrumentation (VI) LabVIEW software to automatically  
99 display and monitor the possible faults occurring within the GCPV plant. A LabVIEW VI is also used to  
100 log the measured power, voltage and current data for the entire GCPV system, more details regarding the  
101 VI LabVIEW structure is presented in [34].

102 The main contribution of this work is the theoretical implementation of a simple, fast and reliable GCPV  
103 fault detection algorithm. The algorithm does not depend on any statistical techniques which makes it  
104 easier to facilitate and detect faults based on theoretical curves analysis and fuzzy logic classification  
105 system. In practice, the proposed fault detection algorithm is capable of localizing and identifying faults  
106 occurring on the DC-side of GCPV systems. The types of fault which can be detected are based on the  
107 size of the GCPV plant, which will be discussed in the next section. The algorithm is based on a six layer  
108 method working sequentially as shown in Fig. 1.

109 This paper is organized as follows: Section 2 describes the methodology used which includes the PV  
110 theoretical power curve modelling and the proposed fault detection algorithm, while section 3 explains  
111 the validation and a brief discussion of the proposed fault detection algorithm. Finally, section 4 describes  
112 the conclusion and future work.

113

## 114 **2. METHODOLOGY**

### 115 **2.1 Photovoltaic Theoretical Power Curve Modelling**

116 The DC side of the GCPV system is modelled using the 5-parameter model. The voltage and current  
117 characteristics of the PV module can be obtained using the single diode model [35] as shown in (1).

$$118 \quad I = I_{ph} - I_o \left( e^{\frac{V+IR_s}{nsV_t}} - 1 \right) - \left( \frac{V+IR_s}{R_{sh}} \right) \quad (1)$$

119 Where  $I_{ph}$  is the photo-generated current at STC ,  $I_o$  is the dark saturation current at STC,  $R_s$  is the  
120 module series resistance,  $R_{sh}$  is the panel parallel resistance,  $ns$  is the number of series cells in the PV  
121 module and  $V_t$  is the thermal voltage and it can be defined based on (2).

$$122 \quad V_t = \frac{AKT}{q} \quad (2)$$

123 Where  $A$  the ideal diode factor,  $k$  is Boltzmann's constant and  $q$  is the charge of the electron.

124 The five parameter model is determined by solving the transcendental equation (1) using Newton-  
125 Raphson algorithm [36] based only on the datasheet of the available parameters for the examined PV  
126 module that was used in this work as shown in Table 1. The power produced by the PV module in Watts  
127 can be easily calculated along with the current (I) and voltage (V) that is generated by equation (1),  
128 therefore:

$$129 \quad P_{\text{theoretical}} = I \times V \quad (3)$$

130 The Power-Voltage (P-V) curve analysis of the tested PV module is shown in Fig. 2. The maximum  
131 power and voltage for each irradiance level under the same temperature value can be expressed by the P-  
132 V curves.

133 The purpose of using the analysis for the P-V curves, is to generate the expected output power of the  
134 examined PV module, therefore, it can be used to predict the error between the measured PV data and the  
135 theoretical power and voltage performance.

136 The proposed PV fault detection algorithm can detect various fault in the GCPV plants such as:

- 137 • Partial shading (PS) condition effects the GCPV system
- 138 • 1 Faulty PV module and PS
- 139 • 2 Faulty PV modules and PS
- 140 • 3 Faulty PV modules and PS
- 141 ○
- 142 ○
- 143 ○
- 144 • (n-1) Faulty PV modules and PS, where n is the total number of PV modules in the GCPV  
145 installation.

146 In this paper, faulty PV module corresponds to a short-circuited PV module. Moreover, A briefly  
147 explanation of the proposed fault detection algorithm is presented in section 2.2 and section 2.3.

## 2.2 *Proposed Fault Detection Algorithm: Theoretical Curves Modelling*

148 The main objective of the fault detection algorithm is to detect and determine when and where a fault has  
149 occurred in the GCPV plant.

150 The first layer of the fault detection algorithm passes the measured irradiance level and photovoltaic  
151 module's temperature to VI LabVIEW software in order to generate the expected theoretical P-V curve as  
152 described previously in section 2.1. This layer is shown in Fig. 3.

153 To determine if a fault has occurred in a GCPV system, two ratios have been identified. The theoretical  
 154 Power ratio (PR) and the theoretical voltage ratio (VR) have been used to categorize the region of the  
 155 fault. It is necessary to use both ratios because:

- 156 1. Both ratios are changeable during faulty conditions in the PV systems
- 157 2. When the power ratio is equal to zero, the voltage ratio can still have a value regarding the  
 158 voltage open circuit of the PV modules

159 The power and voltage ratios are given by the following expressions:

$$160 \quad PR = \frac{P_{G,T}}{P_{G,T} - nP_0} \quad (4)$$

$$161 \quad VR = \frac{V_{G,T}}{V_{G,T} - nV_0} \quad (5)$$

162 Where  $P_{G,T}$  is the theoretical output power generated by the GCPV system at specific G (irradiance) and  
 163 T (module temperature) values,  $n$  is the number of PV modules,  $V_{G,T}$  is the theoretical output voltage  
 164 generated by the GCPV system at specific G (irradiance) and T (module temperature) values and both  
 165  $V_0, P_0$  are the maximum operating voltage and power at STC (G: 1000 W/m<sup>2</sup>, T: 25 °C) respectively.

166 The number of faulty PV modules can be expressed by the number of PV modules in the examined PV  
 167 string. For example, if the PV string comprises 5 photovoltaic modules connected in series, then,  $n = 5$ .

168 In reality, the internal sensors used to measure the voltage and current for a GCPV system have  
 169 efficiencies of less than 100%. This tolerance rate must therefore be considered in the PR and VR ratio  
 170 calculations. For this instance, the PR and VR values are divided into two limits:

- 171 1. High limit: where the maximum operating efficiency of the sensors is applied, therefore, the high  
 172 limit for both PR and VR ratios is expressed by (4) and (5).
- 173 2. Low limit: where the efficiency (tolerance rate) of the sensors is applied. Both limits can be  
 174 expressed by the following formulas:

$$175 \quad PR \text{ Low limit} = \frac{P_{G,T}}{(P_{G,T} - nP_0)\eta_{\text{sensor}}} \quad (6)$$

$$176 \quad VR \text{ Low limit} = \frac{V_{G,T}}{(V_{G,T} - nV_0)\eta_{\text{sensor}1}} \quad (7)$$

177 Where  $\eta_{\text{sensor}}$  is the efficiency of both the voltage and current sensor, while,  $\eta_{\text{sensor}1}$  is the efficiency of  
 178 the voltage sensor:

$$179 \quad \eta_{\text{sensor}} = \eta_{\text{sensor}1}(\text{Voltage Sensor efficiency}) + \eta_{\text{sensor}2}(\text{Current Sensor efficiency}) \quad (8)$$

180 The PR and VR high and low detection limits are evaluated for the examined GCPV system using various  
 181 irradiance levels, as described in the third layer in Fig. 3. For this particular layer, the analysis of the PR  
 182 vs. VR curves can be seen in the example shown next to layer 5, Fig. 3. This example shows the high and  
 183 low detection limit for two case scenarios: one faulty PV module and two faulty PV modules, where both

184 curves are created using 3<sup>rd</sup> order polynomial functions. The purpose of the 3<sup>rd</sup> order polynomial curves is  
185 to generate a regression function which describes the performance of the curves which are created by the  
186 theoretical points using VI LabVIEW software.

187 The overall GCPV fault detecting algorithm is explained in Fig. 3. Layer 5, shows the measured data vs.  
188 the 3<sup>rd</sup> order polynomial curves generated by VI LabVIEW software. The measured PR and measured VR  
189 can be evaluated using the following formula:

$$190 \quad \text{Measured PR vs. Measured VR} = \frac{P_{G,T}}{P_{\text{MEASURED}}} \text{ vs. } \frac{V_{G,T}}{V_{\text{MEASURED}}} \quad (9)$$

191 In case of which the measured PR vs. VR is out of range:

$$192 \quad F \text{ High limit} < \text{Measured PR vs. Measured VR} < F \text{ low limit}$$

193 Therefore, the fault detection algorithm cannot identify the type of the fault that has occurred in the  
194 GCPV plant. However, it can predict two possible faulty conditions which might have occurred in the  
195 GCPV system. As shown in Fig. 3, layer 5 example. The measured data 2 indicates two possible faulty  
196 conditions:

- 197 1. Faulty PV module and PS effects on the GCPV system
- 198 2. Two faulty PV modules and PS effects on the GCPV system

199 Therefore, out of region samples is processed by a fuzzy logic classifier as shown in Fig 3, layer 6.

200 The difference between the proposed theoretical curve modelling with other similar approaches described  
201 by [7, 8, 9 and 10] is that the algorithm contains the number of PV modules in the GCPV system, also the  
202 approach is using 3<sup>rd</sup> order polynomial function which can be used to plot a regression function that  
203 describes the behavior of the faulty region and the design of a fuzzy logic fault classification which is  
204 described in the next section (section 2.3).

### 2.3 Proposed Fault Detection Algorithm: Fuzzy Logic Classifier

205 Nowadays, fuzzy logic systems became more in use with PV systems. A brief overview of the recent  
206 publications on fuzzy logic system design is presented by L. Suganthi [37]. From the literature reviewed  
207 previously in the introduction, currently, there are a lack of research in the field of fuzzy logic  
208 classification systems which are used in examining faulty conditions in PV plants. Therefore, in this  
209 paper, a fuzzy logic classifier is demonstrated and verified experimentally.

210 Fig. 4 describes the overall fuzzy logic classifier system design. The fuzzy logic system consists of two  
211 inputs: voltage ratio (VR) and the power ratio (PR), denoted in Fig. 4 as (A) and (B) respectively. The  
212 membership function for each input is divided into five fuzzy sets described as: PS (partial shading  
213 condition), 1 (one faulty PV module), 2 (two faulty PV modules), 3 (three faulty PV modules) and 4 (four  
214 faulty PV modules). The fuzzy interface applies the approach of Mamdani method (min-max) managed  
215 by the fuzzy logic system rule, stage 2 of the fuzzy logic system. After the rules application, the output is  
216 applied to classify the fault detection type occurred in the GCPV plant.

217 A brief calculation of each membership function for VR, PR and the fuzzy logic membership output  
218 function is reported in Fig. 5. The membership functions are based on the mathematical calculation of the  
219 examined GCPV plant used in this work. The examined GCPV system which is used to evaluate the  
220 performance of the fault detection algorithm is demonstrated briefly in section 3.1: experimental setup.

221 Both fuzzy logic system inputs VR and PR are evaluated at the maximum power and voltage of the  
222 GCPV system which are equal to 1100Wp and 143.5V. In addition, the mathematical calculations  
223 includes the PS conditions which might affect the performance of the entire PV system.

224 The fuzzy logic system rule are based on: if, and statement. Each case scenario is presented after the  
225 fuzzy logic system rule as shown in Fig. 5. However, the output membership function is divided into 5  
226 sets: PS (0 - 0.2), faulty PV module (0.2 – 0.4), two faulty PV modules (0.4 – 0.6), three faulty PV  
227 modules (0.6 – 0.8) and four faulty PV modules (0.8 – 1.0).

228 Furthermore, the output surface for the fuzzy logic classifier system is plotted and presented by a 3D  
229 fitting curve shown in Fig. 6. Where the x-axis presents the PR, y-axis presents VR and the fault detection  
230 output classification is on the z-axis.

231 In order to generalize the proposed fuzzy logic classification systems, it is required to input the values of  
232 the voltage and the power to the fuzzy interface system, and then, the faulty region could be calculated  
233 using the formulas (4 & 5) for the variations of the power and voltage respectively. Additionally, the  
234 output detection membership function could be extended up to the value of the PV modules connected in  
235 series in each PV string separately and this extension in the membership function can be evaluated within  
236 the region of 0 to 1 as the following:

237 
$$1 / \text{number of series PV modules in the PV string}$$

### 238 3. *GCPV Fault Detection Algorithm Validation*

239 In this section, the performance of the proposed fault detection algorithm is verified. For this purpose, the  
240 acquired data for various days have been considered using 1.1 kWp GCPV plant. The time zone for all  
241 measurements is GMT.

#### 242 3.1 *Experimental Setup*

243 The PV system used in this work consists of a GCPV plant comprising 5 polycrystalline silicon PV  
244 modules each with a nominal power of 220 Wp. The PV modules are connected in series. The PV string  
245 is connected to a Maximum Power Point Tracker (MPPT) with an output efficiency of not less than 95%.  
246 The DC current and voltage are measured using the internal sensors which are part of the FLEXmax  
247 MPPT unit. A battery bank is used to store the energy produced by the PV plant.

248 A Vantage Pro monitoring unit is used to receive the Global solar irradiance measured by the Davis  
249 weather station which includes a pyranometer. A Hub 4 communication manager is used to facilitate  
250 acquisition of modules' temperature using the Davis external temperature sensor, and the electrical data  
251 for each PV string. VI LabVIEW software is used to implement data logging and monitoring functions of  
252 the GCPV system. Fig. 7 illustrates the overall system architecture of the GCPV plant.

253 The real-time measurements are taken by averaging 60 samples, gathered at a rate of 1Hz over a period of  
254 one minute. Therefore, the obtained results for power, voltage and current are calculated at one minute  
255 intervals.

256 The SMT6 (60) P solar module manufactured by Romag, has been used in this work. The electrical  
257 characteristics of the solar module are shown in Table 1. The standard test condition (STC) for these solar  
258 panels are: Solar Irradiance = 1000 W/m<sup>2</sup>, Module Temperature = 25 °C.



259 The fault detection algorithm has been validated experimentally over a 5 day period. On each day a  
260 different fault case scenario was perturbed as shown in Fig. 8:

- 261 1. Day1: Normal operation mode and PS effects on the GCPV plant (no fault occurred in any of the  
262 tested PV modules),
- 263 2. Day2: One faulty PV module and PS effects on the GCPV plant
- 264 3. Day3: Two faulty PV modules and PS effects on the GCPV plant
- 265 4. Day4: Three faulty PV modules and PS effects on the GCPV plant
- 266 5. Day5: Four faulty PV modules and PS effects on the GCPV plant

267 In all cases, faulty PV module stands for an in active PV module which means that this particular PV  
268 module has been disconnected (short circuit) from the entire examined PV plant.

269 In order to test the effectiveness of the proposed fault detection algorithm, the theoretical and the  
270 measured output power for each case scenario was logged and compared using VI LabVIEW software.

### 271 3.2 Evaluation of the Proposed Theoretical Curves Modelling

272 In this section, the performance of the fault detection algorithm (theoretical curves modelling) is verified  
273 using normal operation mode and partial shading effects the GCPV system. Fig. 9 describes the  
274 theoretical simulation vs. real time long term data measurement.

275 In order to apply a partial shading condition to the GPCV modules an opaque paper object has been used.  
276 The partial shading was applied to all PV modules at the same rate. Partial shading condition is increased  
277 during the test. In case of overcast scenario affecting the PV modules, the performance of the entire  
278 system will remain with a consistent output power, therefore, the faults or PS conditions could be  
279 identified using the purposed algorithm.

280 Fig. 10(A) shows the entire measured data vs. theoretical detection limits which are discussed previously  
281 in section 2.2. As can be noticed, most of the measured data lies within the high and low theoretical  
282 detection limits which are created using 3<sup>rd</sup> order polynomial function. The high and low detection limit  
283 functions are also illustrated in the Fig 10(A).

284 PR and VR ratios for this particular test is shown in Fig 10(B). Since the PS condition applied to the  
285 GCPV system is increasing, therefore, both VR and PR ratios are increasing slightly during the test.  
286 Moreover, both ratios can be measured using (9). Fig. 10(B) shows the efficiency of the GCPV plant.  
287 The efficiency is evaluated using (10).

$$288 \quad \text{Efficienecy} = \frac{\text{Measured Output Power}}{\text{Theoretical Power}} \quad (10)$$

289 From Fig. 10(B), the efficiency of the GCPV system decreased while increasing the PS applied to the PV  
290 system. The detection accuracy (DA) for the proposed theoretical curves modelling algorithm is  
291 calculated using (11).

$$292 \quad \text{Detection accuracy (DA)} = \frac{\text{Total Number of Samples} - \text{Out of Region Samples}}{\text{Total Number of Samples}} \quad (11)$$

293 Using (11), the proposed algorithm has a detection accuracy equals to:

294 
$$\text{Detection accuracy for the partial shading condtion} = \frac{720 - 37}{720} = 0.9486 = 94.86\%$$

295 In this test, the theoretical curves modelling fault detection algorithm shows a significant success for  
296 detecting partial shading conditions applied to the GCPV plant. The detection accuracy rate can be  
297 increased using a fuzzy logic classification system. Therefore, out of region samples (samples which are  
298 away from the high and low detection limits) are processed by the fuzzy logic system.

299 In this paper, the MPPT unit is used to locate and acquired the output power at the global maximum  
300 power point (GMPP), therefore, all local maximum power points (LMPP) are not considered in the fault  
301 detection algorithm. Fig. 11(A) illustrates one examined case scenario which shows the percentage of the  
302 partial shading on each examined PV module. The output P-V curve of the PV system is shown in Fig.  
303 11(B). As can be noticed, the MPPT unit locates all LMPP and GMPP, however, the output of the MPPT  
304 unit is at the GMPP.

305 In order to detect all LMPPs and the GMPP obtained by the MPPT unit, it is required to further  
306 investigate MPPT techniques which is not one of the targets of this manuscript.

### 307 **3.3 Evaluation of the Proposed Fuzzy Logic Classification System**

308 This test is created to confirm the ability of the fault detection algorithm to detect faulty PV modules  
309 occurring in the GCPV plant using theoretical curves modelling algorithm and fuzzy logic classification  
310 system. Four different case scenarios have been tested:

- 311 A. Faulty PV module with partial shading condition
- 312 B. Two faulty PV modules with partial shading condition
- 313 C. Three faulty PV modules with partial shading condition
- 314 D. Four faulty PV module and partial shading condition

315 Each case scenario is examined during a time period of a full day as shown Fig. 8 (Day 2, 3, 4 and 5),  
316 where the total number of samples for each examined day are equal to 720 samples. Fig. 10 shows the  
317 theoretical curve limits vs. real-time long-term measured data. 3<sup>rd</sup> order polynomial function of the  
318 theoretical high and low limits is plotted, while the minimum determination factor (R) is equal to 99.59%.

319 As can be noticed, the measured data for each test is plotted and compared with the theoretical curve  
320 limits. Most of the measured data among the 4 day test period lies within the high and low detection  
321 limits of the theoretical curves. However, in each day, several out of region samples have been detected as  
322 shown in Fig. 12.

323 The detection accuracy (DA) for each case scenario is calculated using (11) and reported in Table 2. The  
324 minimum and maximum DA is equal to 94.03% and 95.27% respectively before considering the fuzzy  
325 logic classification system.

326 For each test including the test illustrated in section 3.2, out of region samples have been processed by the  
327 fuzzy logic classification system. Fig. 13 describes the performance of the fuzzy logic system during each  
328 test:

- 329 • Test 1: PS, described in section 3.2
- 330 • Test 2: One faulty PV module and PS
- 331 • Test 3: Two faulty PV modules and PS
- 332 • Test 4: Three faulty PV modules and PS
- 333 • Test 5: Four faulty PV modules and PS

334 It is evident that most of the samples are categorized correctly by the fuzzy classifier. For example, before  
335 considering the fuzzy logic system, the DA for test 2 is equal to 95.27% while the DA increased up to  
336 99.03% after taking into account the fuzzy logic classification system. This result is due to the detection  
337 of the out of region samples. The results for this test is shown in Fig. 13, only 7 out of 34 processed  
338 samples are detected incorrectly, while 27 samples have been detected correctly within an output  
339 membership function between 0.2 and 0.4.

340 Table 2 shows number of out of region samples and the detection accuracy (DA) for each test separately.  
341 The DA rate is increased up to a minimum value equals to 98.8%.

342 In this section, the evaluation for the theoretical curves modelling algorithm and the fuzzy logic system  
343 are discussed and briefly explained. From the obtained results, it is confirmed that the fault detection  
344 algorithm proposed in this article is suitable for detecting faulty conditions in PV systems accurately.

#### 345 **3.4 Evaluation of the Proposed Method Using Hot Spot Detection in PV Modules**

346 This test is created to confirm the ability of the fault detection algorithm to detect hot spots in PV  
347 modules. The test was evaluated using two different PV modules which contains different hot spots. As  
348 shows in Fig. 14(A), the first PV module contains only one hot spot in the top right side of the PV  
349 module, however, the second tested PV module contains two adjacent hot spots. The thermal images were  
350 taken from FLIR i7 camera, which has a thermal sensitivity equals to 0.1 °C (32.18 °F).

351 The first PV module temperature is measured at 55.4 °F, while the hot spot has been detected at 60.2 °F.  
352 Same results obtained for the second PV module where the PV module temperature is approximately  
353 equals to 56.8 °F. However, the hot spots detected in the PV module have a temperature equal to 59.6 °F  
354 and 62.3 °F.

355 The theoretical curves modelling was used to evaluate the difference between a healthy PV module (PV  
356 module without hot spots) with the examined PV modules shown in Fig. 14(A) at the same environmental  
357 conditions. The results of this test is shown in Fig. 14(B). As can be noticed, the detection limits of the  
358 theoretical curves does only contain most of the PV data obtained from the healthy PV module.  
359 Furthermore, the measured data of the first PV module which contains only one hot spot shows an  
360 increase in the values of the PR and VR. This results is due to the decrease in the value of the voltage  
361 obtained from the PV module. The voltage from this particular PV module is decreased approximately  
362 about 2V. Therefore the overall VR and PR is increased as can be demonstrated by (12).

363 The second PV module has more drop in the value of the voltage due to the detection of two hot spots.  
364 The drop in the value of the voltage is estimated at 3.7V. As shown in Fig. 14(B), the measured data  
365 obtained from the second PV module show a significant increase in the values of the VR and PR.  
366 Therefore, the measured data is apart from the detection limits obtained by the fault detection algorithm.

367 
$$\uparrow \text{VR} = \frac{V_{G,T \text{ theoretical}}}{\downarrow V_{G,T \text{ measured}} - nV_0} \quad \& \quad \uparrow \text{PR} = \frac{P_{G,T \text{ theoretical}}}{\downarrow P_{G,T \text{ measured}} - nP_0} \quad (12)$$

368 **3.5 Discussion**

369 In order to test the effectiveness of the proposed fault detection algorithm presented in this paper, the  
 370 results obtained have been compared with multiple fault detection approaches. The common combination  
 371 between the proposed algorithm in this paper and the research demonstrated by [5, 8 and 38-39] is the VR  
 372 and PR equations. However, the VR and PR equations presented in this work have a different parameters  
 373 such as:

- 374 1. VR and PR equations contain the number of modules that are examined in the GCPV plant,  
 375 which is presented using the variable: n.
- 376 2. Both equations contain the voltage and current sensors uncertainly (sensor efficiency rate), which  
 377 makes the algorithm easier to use with different PV installations.
- 378 3. The detection limits (high and low) is a novel idea which has not been presented by any other  
 379 research article related to fault detection algorithms in PV systems.

380 Moreover, by using VR and PR ratios it was evident that the algorithm can detect up to (n-1) faulty PV  
 381 modules and PS effects the GCPV plant, where n is equal to the number of PV modules in the examined  
 382 GCPV installation. In this paper, a MPPT unit which has an output power of one single point (mostly, it is  
 383 equal to the GMPP), therefore, the detection algorithm is not capable of detecting and categorizing ALL  
 384 LMPP, since the examined PV system is using a MPPT unit without any enhancement of the output  
 385 power using an advanced MPPT techniques.

386 In [7 and 12] statistical analysis technique based on standard divination limits are used to detect possible  
 387 faults in the GCPV plant, however, the presented techniques cannot identify the type of the fault occurred  
 388 in the PV system, therefore, it is necessary to create a new mathematical calculations of the entire GCPV  
 389 plant. In this paper, it is presented that the algorithm is based on the analysis of the theoretical curves  
 390 modelling using 3<sup>rd</sup> order polynomial functions, without the use of any statistical analysis approaches.

391 Furthermore, [10] experimented another statistical analysis technique called t-test. This algorithm is  
 392 capable to detect multiple faults in PV systems, however, the ratios used to monitor the performance of  
 393 the PV system does not contain any parameter for the number of PV modules and the uncertainly in the  
 394 internal voltage and current sensors used.

395 There are variety of fuzzy logic control systems used with PV applications. Three-phase three-level grid  
 396 interactive inverter with fuzzy based maximum power point tracking controller is presented by [40].  
 397 Additionally, some of the fuzzy logic classification systems were used with hybrid green power systems  
 398 as reported by S. Safari et al [41]. Furthermore, M. Tadj et al [5] presented a fuzzy logic technique which  
 399 is used to estimate the solar radiation, the proposed technique contains three membership functions:  
 400 cloudy sky, partial cloudy sky and clear sky. However, in this paper, a new attempt for using fuzzy logic  
 401 classification system to detect possible faults occurring in the PV plans. The main purpose of the fuzzy  
 402 logic presented in this work is to detect out of region samples (samples that lies away from the high and  
 403 low theoretical detection limits), and therefore, to increase the detection accuracy of the fault detection  
 404 algorithm. The fuzzy logic system can be reused with other GCPV plants by changing the parameters  
 405 which are shown in Fig. 5.

406 Overall comparison between this work and the research presented by [4, 7 & 8] are listed in Table 3. As  
407 can be seen that this work is the only research contains a mathematical modelling technique (3<sup>rd</sup> order  
408 polynomial functions) presented previously in Layer 3, Fig 3. Also this paper demonstrates a new  
409 statistical technique which can be used in the detection of faulty conditions in PV systems called t-test  
410 statistical method. Comparing to [4, 7 and 8], the proposed fault detection algorithm presented in this  
411 research can detects all type of faults listed in Table 3 including: partial shading conditions, faulty PV  
412 modules and evaluating the hot spots in PV modules. However, the algorithm cannot distinguish between  
413 the investigated partial shading conditions occurred in the PV modules and hot spots.

414 The fault detection algorithm presented in this work contains some advantages and disadvantages such as:

#### 415 **Advantages:**

- 416 • The fault detection algorithm can be used with wide range of PV installation, since it depends on  
417 the analysis of the power and the voltage ratios.
- 418 • Multiple faults can be detected accurately, the minimum and maximum detection accuracy  
419 obtained by the algorithm are equal to 98.8% and 99.31% respectively.
- 420 • The efficiency of the voltage and current sensor has been taken into account in the mathematical  
421 modelling for the proposed fault detection algorithm.
- 422 • The fuzzy logic classification system is easy to be reused in other PV systems since it depends  
423 only on the analysis of the VR and PR.
- 424 • Hot spot detection can also be evaluated using the proposed theoretical curves modelling.

#### 425 **Disadvantages:**

- 426 • The algorithm depends on the voltage and the power ratios of the GCPV systems. Therefore, the  
427 accuracy of the algorithm depends on the instrumentation used in the PV plants.
- 428 • The algorithm is not capable of detecting faults occurring in the bypass diodes, which are  
429 commonly used nowadays with PV systems. This problem in PV plants has been investigated by  
430 W. Chine et al [9], M. Duong et al [42] & S. Silvestre et al [43].
- 431 • The fault detection algorithm cannot detect any fault arising in the DC/AC inverter units which  
432 are commonly used with GCPV systems. This type of fault has been reported by M. Dhimish et al  
433 [12], G. Bayrak [23] and F. Deng et al [44].

#### 434 **4. Conclusion**

435 In this work, a new GCPV fault detection algorithm is proposed. The developed fault detection algorithm  
436 is capable of detecting faulty PV modules and partial shading conditions which affect GCPV systems.  
437 The detection algorithm has been tested using 1.1kWp GCPV system installed at Huddersfield University,  
438 United Kingdom.

439 The fault detection algorithm consist of six layers working in series. The first layer contains the input  
440 parameters of the sun irradiance and PV modules' temperature, while the second layer generates the  
441 GCPV theoretical performance analysis using Virtual Instrumentation (VI) LabVIEW software. Layer 3  
442 identifies the power and voltage ratios, subsequently creates a high and low detection limits which will be  
443 used in Layer 4 to apply the 3<sup>rd</sup> order polynomial regression model on the top of the PR and VR ratios.  
444 The fifth layer consists of two parts: the input parameters of the examined GCPV systems and the 3<sup>rd</sup>  
445 order polynomial detection limits. If the measured voltage ratio vs. measured power ratio lies away from

446 the detection limits, the samples will be processed by the last layer which contains the fuzzy logic  
447 classification system.

448 The novel contribution of this research is that the fault detection algorithm depends on the variations of  
449 the voltage and the power of the GCPV plant. Additionally, the PR and VR equations contains the  
450 number of examined modules and the uncertainly of the voltage and current sensors used. Also, there are  
451 a few fuzzy logic classification systems which are used with PV fault detection algorithms, therefore, this  
452 research introduced a simple, reliable and quick fuzzy logic classification system which can be reused  
453 with various GCPV plants. Finally, the PV theoretical curves modelling can be used to evaluate PV  
454 modules which contain hot spots.

455 The results indicate that the fault detection algorithm is detecting most of the measured data within the  
456 theoretical limits created using 3<sup>rd</sup> order polynomial functions. Furthermore, the maximum detection  
457 accuracy of the algorithm before considering the fuzzy logic system is equal to 95.27%, however, the  
458 fault detection accuracy is increased up to a minimum value of 98.8% after considering the fuzzy logic  
459 system.

460 In future, it is intended to implement the proposed fault detection technique on a low cost microcontroller  
461 based system. The system's fault detection capabilities will be enhanced further by using artificial  
462 intelligence machine learning technique to predict possible faults occurring in the GCPV system using  
463 artificial neural networks (ANN).

#### 464 **References**

- 465 [1] Bortolini, M., Gamberi, M., & Graziani, A. (2014). Technical and economic design of photovoltaic and  
466 battery energy storage system. *Energy Conversion and Management*, 86, 81-92.
- 467 [2] Dhimish, M., Holmes, V., Mehrdadi, B., Dales, M., Chong, B., & Zhang, L. (2017). Seven indicators  
468 variations for multiple PV array configurations under partial shading and faulty PV conditions. *Renewable*  
469 *Energy*.
- 470 [3] Kadri, R., Andrei, H., Gaubert, J. P., Ivanovici, T., Champenois, G., & Andrei, P. (2012). Modeling of the  
471 photovoltaic cell circuit parameters for optimum connection model and real-time emulator with partial  
472 shadow conditions. *Energy*, 42(1), 57-67.
- 473 [4] Dhimish, M., Holmes, V., Mehrdadi, B., & Dales, M. (2017). Diagnostic method for photovoltaic systems  
474 based on six layer detection algorithm. *Electric Power Systems Research*, 151, 26-39.
- 475 [5] Tadj, M., Benmouiza, K., Cheknane, A., & Silvestre, S. (2014). Improving the performance of PV systems  
476 by faults detection using GISTEL approach. *Energy conversion and management*, 80, 298-304.
- 477 [6] Takashima, T., Yamaguchi, J., Otani, K., Oozeki, T., Kato, K., & Ishida, M. (2009). Experimental studies  
478 of fault location in PV module strings. *Solar Energy Materials and Solar Cells*, 93(6), 1079-1082.
- 479 [7] Chouder, A., & Silvestre, S. (2010). Automatic supervision and fault detection of PV systems based on  
480 power losses analysis. *Energy Conversion and Management*, 51(10), 1929-1937.
- 481 [8] Silvestre, S., Kichou, S., Chouder, A., Nofuentes, G., & Karatepe, E. (2015). Analysis of current and  
482 voltage indicators in grid connected PV (photovoltaic) systems working in faulty and partial shading  
483 conditions. *Energy*, 86, 42-50.
- 484 [9] Chine, W., Mellit, A., Lughy, V., Malek, A., Sulligoi, G., & Pavan, A. M. (2016). A novel fault diagnosis  
485 technique for photovoltaic systems based on artificial neural networks. *Renewable Energy*, 90, 501-512.

- 486 [10] Dhimish, M., & Holmes, V. (2016). Fault detection algorithm for grid-connected photovoltaic plants. *Solar*  
487 *Energy*, 137, 236-245.
- 488 [11] Dhimish, M., Holmes, V., Mehrdadi, B., & Dales, M. (2017). Multi-Layer Photovoltaic Fault Detection  
489 Algorithm. *High Voltage*.
- 490 [12] Dhimish, M., Holmes, V., Mehrdadi, B., & Dales, M. (2017). Simultaneous Fault Detection Algorithm for  
491 Grid-Connected Photovoltaic Plants. *IET Renewable Power Generation*.
- 492 [13] Kim, K. A., Seo, G. S., Cho, B. H., & Krein, P. T. (2016). Photovoltaic Hot-Spot Detection for Solar Panel  
493 Substrings Using AC Parameter Characterization. *IEEE Transactions on Power Electronics*, 31(2), 1121-  
494 1130.
- 495 [14] Dhimish, M., Holmes, V., Mehrdadi, B., & Dales, M. (2017). The Impact of Cracks on Photovoltaic Power  
496 Performance. *Journal of Science: Advanced Materials and Devices*.
- 497 [15] Obi, M., & Bass, R. (2016). Trends and challenges of grid-connected photovoltaic systems—A  
498 review. *Renewable and Sustainable Energy Reviews*, 58, 1082-1094.
- 499 [16] Alam, M. K., Khan, F., Johnson, J., & Flicker, J. (2015). A Comprehensive Review of Catastrophic Faults  
500 in PV Arrays: Types, Detection, and Mitigation Techniques. *IEEE Journal of Photovoltaics*, 5(3), 982-997.
- 501 [17] Khamis, A., Shareef, H., Bizkevelci, E., & Khatib, T. (2013). A review of islanding detection techniques  
502 for renewable distributed generation systems. *Renewable and sustainable energy reviews*, 28, 483-493.
- 503 [18] Boukenoui, R., Salhi, H., Bradai, R., & Mellit, A. (2016). A new intelligent MPPT method for stand-alone  
504 photovoltaic systems operating under fast transient variations of shading patterns. *Solar Energy*, 124, 124-  
505 142.
- 506 [19] Mutlag, A. H., Shareef, H., Mohamed, A., Hannan, M. A., & Abd Ali, J. (2014). An improved fuzzy logic  
507 controller design for PV inverters utilizing differential search optimization. *International Journal of*  
508 *Photoenergy*, 2014.
- 509 [20] Belaout, A., Krim, F., & Mellit, A. (2016, November). Neuro-fuzzy classifier for fault detection and  
510 classification in photovoltaic module. In *Modelling, Identification and Control (ICMIC), 2016 8th*  
511 *International Conference on* (pp. 144-149). IEEE.
- 512 [21] Grichting, B., Goette, J., & Jacomet, M. (2015, June). Cascaded fuzzy logic based arc fault detection in  
513 photovoltaic applications. In *Clean Electrical Power (ICCEP), 2015 International Conference on* (pp. 178-  
514 183). IEEE.
- 515 [22] Chen, J. L., Kuo, C. L., Chen, S. J., Kao, C. C., Zhan, T. S., Lin, C. H., & Chen, Y. S. (2016). DC-Side  
516 Fault Detection for Photovoltaic Energy Conversion System Using Fractional-Order Dynamic-Error-based  
517 Fuzzy Petri Net Integrated with Intelligent Meters. *IET Renewable Power Generation*.
- 518 [23] Bayrak, G. (2015). A remote islanding detection and control strategy for photovoltaic-based distributed  
519 generation systems. *Energy Conversion and Management*, 96, 228-241.
- 520 [24] Rezgui, W., Mouss, L. H., Mouss, N. K., Mouss, M. D., & Benbouzid, M. (2014, March). A smart  
521 algorithm for the diagnosis of short-circuit faults in a photovoltaic generator. In *Green Energy, 2014*  
522 *International Conference on* (pp. 139-143). IEEE.
- 523 [25] Zhao, Y., Ball, R., Mosesian, J., de Palma, J. F., & Lehman, B. (2015). Graph-based semi-supervised  
524 learning for fault detection and classification in solar photovoltaic arrays. *IEEE Transactions on Power*  
525 *Electronics*, 30(5), 2848-2858.

- 526 [26] Zhao, Y., Yang, L., Lehman, B., de Palma, J. F., Mosesian, J., & Lyons, R. (2012, February). Decision  
527 tree-based fault detection and classification in solar photovoltaic arrays. In *Applied Power Electronics*  
528 *Conference and Exposition (APEC), 2012 Twenty-Seventh Annual IEEE* (pp. 93-99). IEEE.
- 529 [27] Shahbazi, M., Jamshidpour, E., Poure, P., Saadate, S., & Zolghadri, M. R. (2013). Open-and short-circuit  
530 switch fault diagnosis for nonisolated dc–dc converters using field programmable gate array. *IEEE*  
531 *transactions on industrial electronics*, 60(9), 4136-4146.
- 532 [28] Rezgui, W., Mouss, H., Mouss, N., Mouss, D., Benbouzid, M., & Amirat, Y. (2015, June). Photovoltaic  
533 module simultaneous open-and short-circuit faults modeling and detection using the I–V characteristic. In  
534 *Industrial Electronics (ISIE), 2015 IEEE 24th International Symposium on* (pp. 855-860). IEEE.
- 535 [29] Chouder, A., Silvestre, S., Taghezouit, B., & Karatepe, E. (2013). Monitoring, modelling and simulation of  
536 PV systems using LabVIEW. *Solar Energy*, 91, 337-349.
- 537 [30] Yadav, Y., Roshan, R., Umashankar, S., Vijayakumar, D., & Kothari, D. P. (2013, April). Real time  
538 simulation of solar photovoltaic module using labview data acquisition card. In *Energy Efficient*  
539 *Technologies for Sustainability (ICEETS), 2013 International Conference on* (pp. 512-523). IEEE.
- 540 [31] Abdulkadir, M., Samosir, A. S., & Yatim, A. H. M. (2013). Modeling and simulation of a solar  
541 photovoltaic system, its dynamics and transient characteristics in LABVIEW. *International Journal of*  
542 *Power Electronics and Drive Systems*, 3(2), 185.
- 543 [32] Blaifi, S., Moulahoum, S., Colak, I., & Merrouche, W. (2017). Monitoring and enhanced dynamic  
544 modeling of battery by genetic algorithm using LabVIEW applied in photovoltaic system. *Electrical*  
545 *Engineering*, 1-18.
- 546 [33] Dhimish, M., Holmes, V., & Dales, M. (2016, September). Grid-connected PV virtual instrument system  
547 (GCPV-VIS) for detecting photovoltaic failure. In *Environment Friendly Energies and Applications*  
548 *(EFEA), 2016 4th International Symposium on* (pp. 1-6). IEEE.
- 549 [34] Dhimish, M., Holmes, V., & Dales, M. (2017). Parallel fault detection algorithm for grid-connected  
550 photovoltaic plants. *Renewable Energy*, 113, 94-111.
- 551 [35] McEvoy, A., Castaner, L., Markvart, T., 2012. Solar Cells: Materials, Manufacture and Operation.  
552 Academic Press.
- 553 [36] Sera, D., Teodorescu, R., & Rodriguez, P. (2007). PV panel model based on datasheet values. Paper  
554 presented at the 2392-2396. doi:10.1109/ISIE.2007.4374981.
- 555 [37] Suganthi, L., Iniyar, S., & Samuel, A. A. (2015). Applications of fuzzy logic in renewable energy systems—  
556 a review. *Renewable and Sustainable Energy Reviews*, 48, 585-607.
- 557 [38] Chine, W., Mellit, A., Pavan, A. M., & Kalogirou, S. A. (2014). Fault detection method for grid-connected  
558 photovoltaic plants. *Renewable Energy*, 66, 99-110.
- 559 [39] Dhimish, M., Holmes, V., Dales, M., Mather, P., Sibley, M., Chong, B., & Zhang, L. (2017, June). Fault  
560 detection algorithm for multiple GCPV array configurations. In *PowerTech, 2017 IEEE Manchester* (pp. 1-  
561 6). IEEE.
- 562 [40] Altin, N., & Ozdemir, S. (2013). Three-phase three-level grid interactive inverter with fuzzy logic based  
563 maximum power point tracking controller. *Energy Conversion and Management*, 69, 17-26.
- 564 [41] Safari, S., Ardehali, M. M., & Sirizi, M. J. (2013). Particle swarm optimization based fuzzy logic controller  
565 for autonomous green power energy system with hydrogen storage. *Energy conversion and*  
566 *management*, 65, 41-49.



- 567 [42] Duong, M. Q., Sava, G. N., Ionescu, G., Necula, H., Leva, S., & Mussetta, M. (2017, June). Optimal bypass  
568 diode configuration for PV arrays under shading influence. In *Environment and Electrical Engineering and*  
569 *2017 IEEE Industrial and Commercial Power Systems Europe (EEEIC/I&CPS Europe), 2017 IEEE*  
570 *International Conference on* (pp. 1-5). IEEE.
- 571 [43] Silvestre, S., Boronat, A., & Chouder, A. (2009). Study of bypass diodes configuration on PV modules.  
572 *Applied Energy*, 86(9), 1632-1640.
- 573 [43] Deng, F., Chen, Z., Khan, M. R., & Zhu, R. (2015). Fault detection and localization method for modular  
574 multilevel converters. *IEEE Transactions on Power Electronics*, 30(5), 2721-2732.

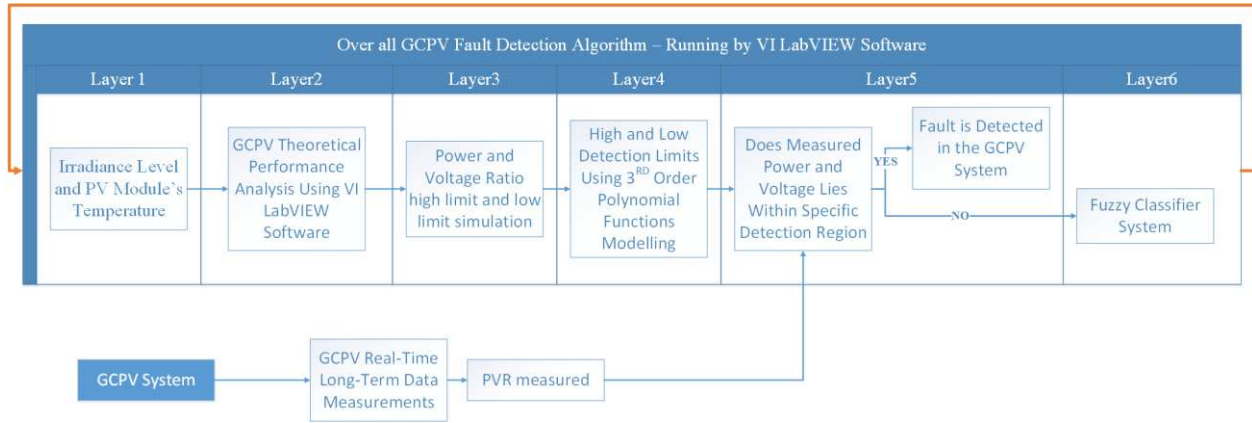


Fig. 1. Over all GCPV fault detection algorithm Layers

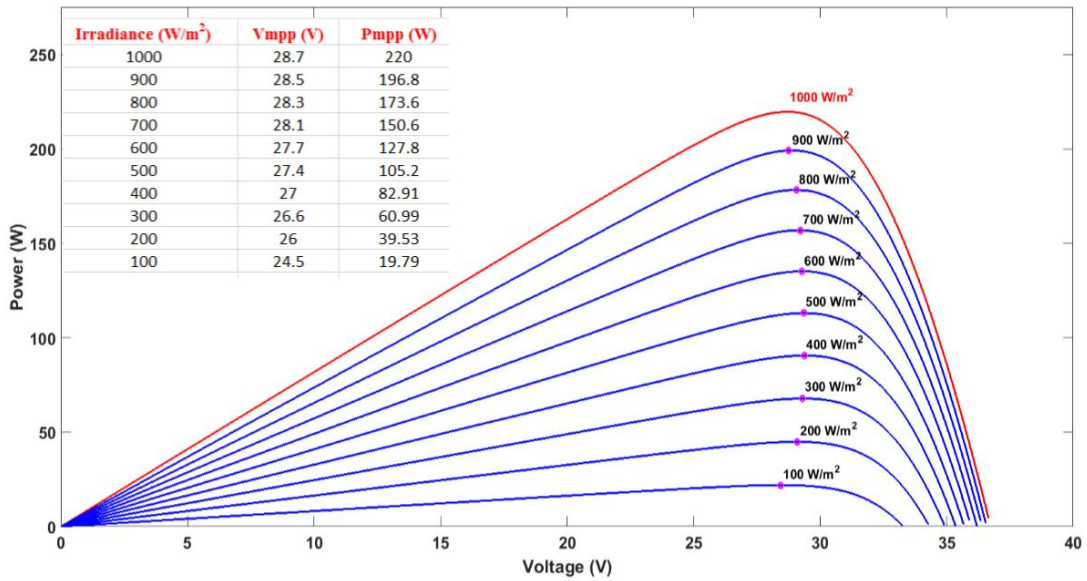


Fig. 2. P-V curve modelling under various irradiance levels

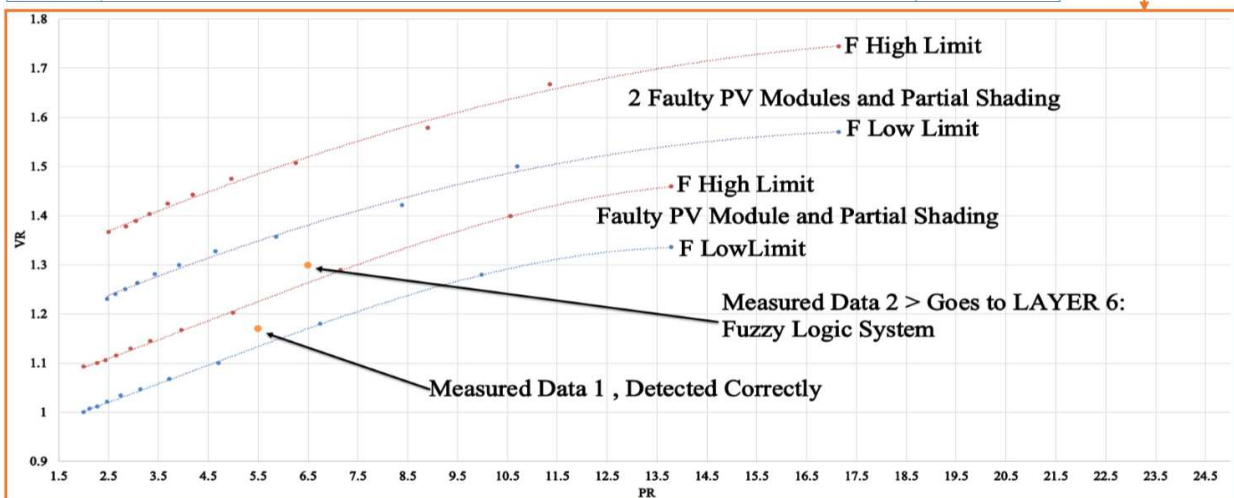
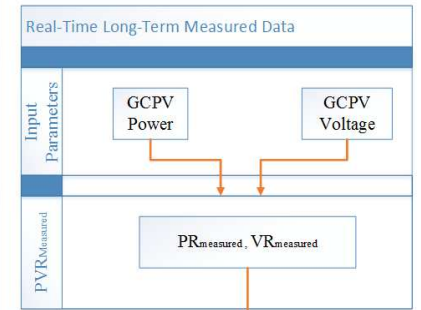
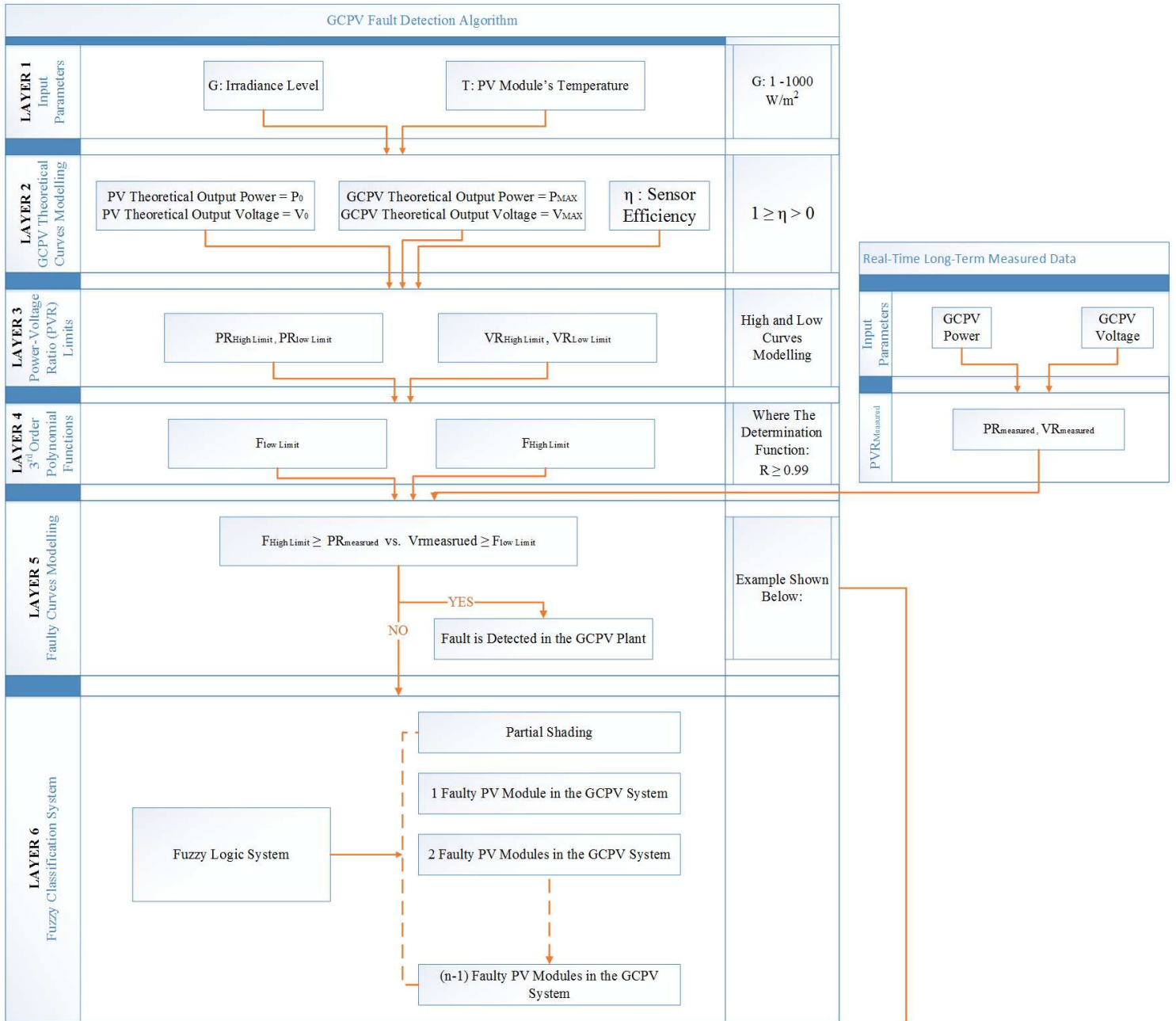


Fig. 3. Detailed flowchart for the proposed fault detection algorithm which contains 5 layers

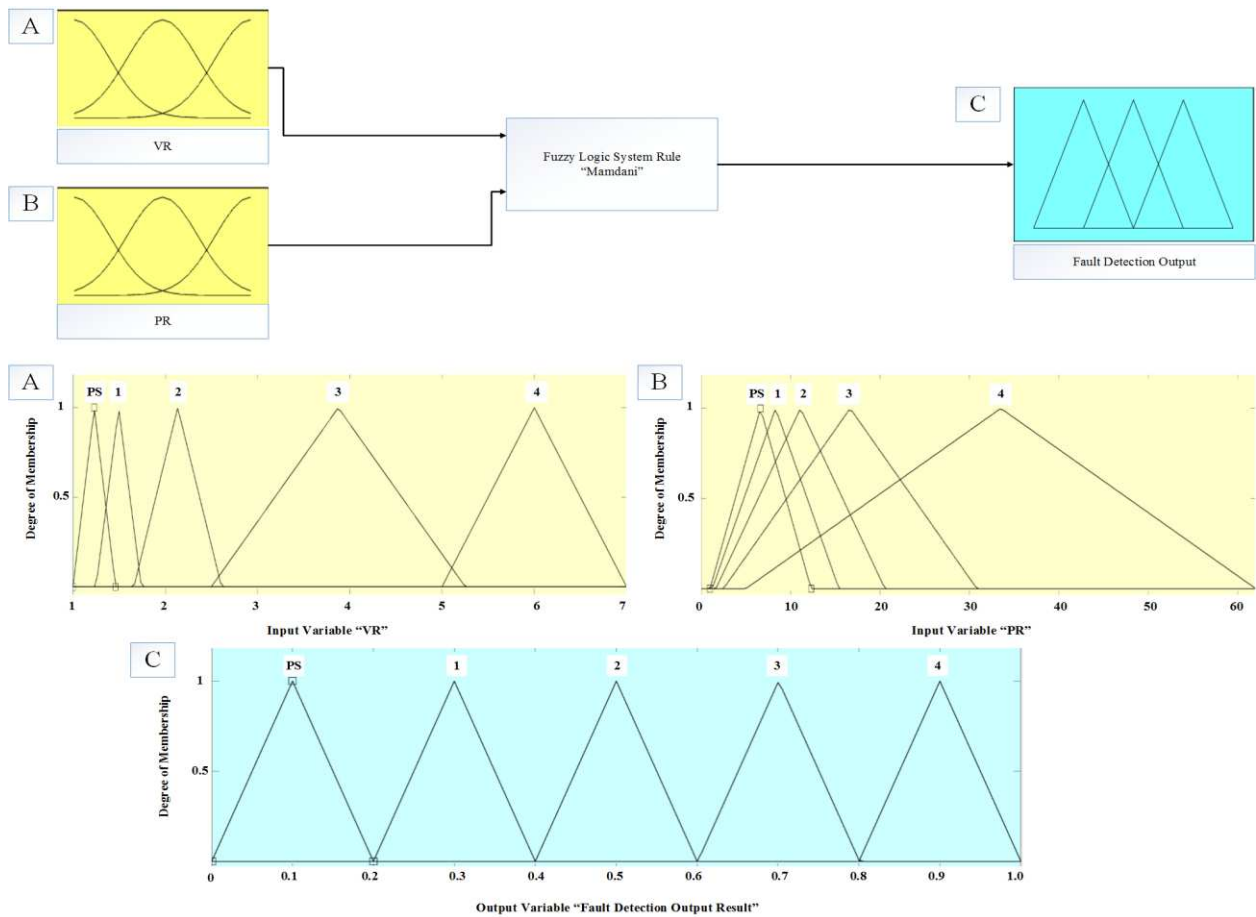


Fig. 4. Fuzzy Logic classifier system design. (A) Voltage ratio input, (B) Power ratio input, (C) Fault detection output

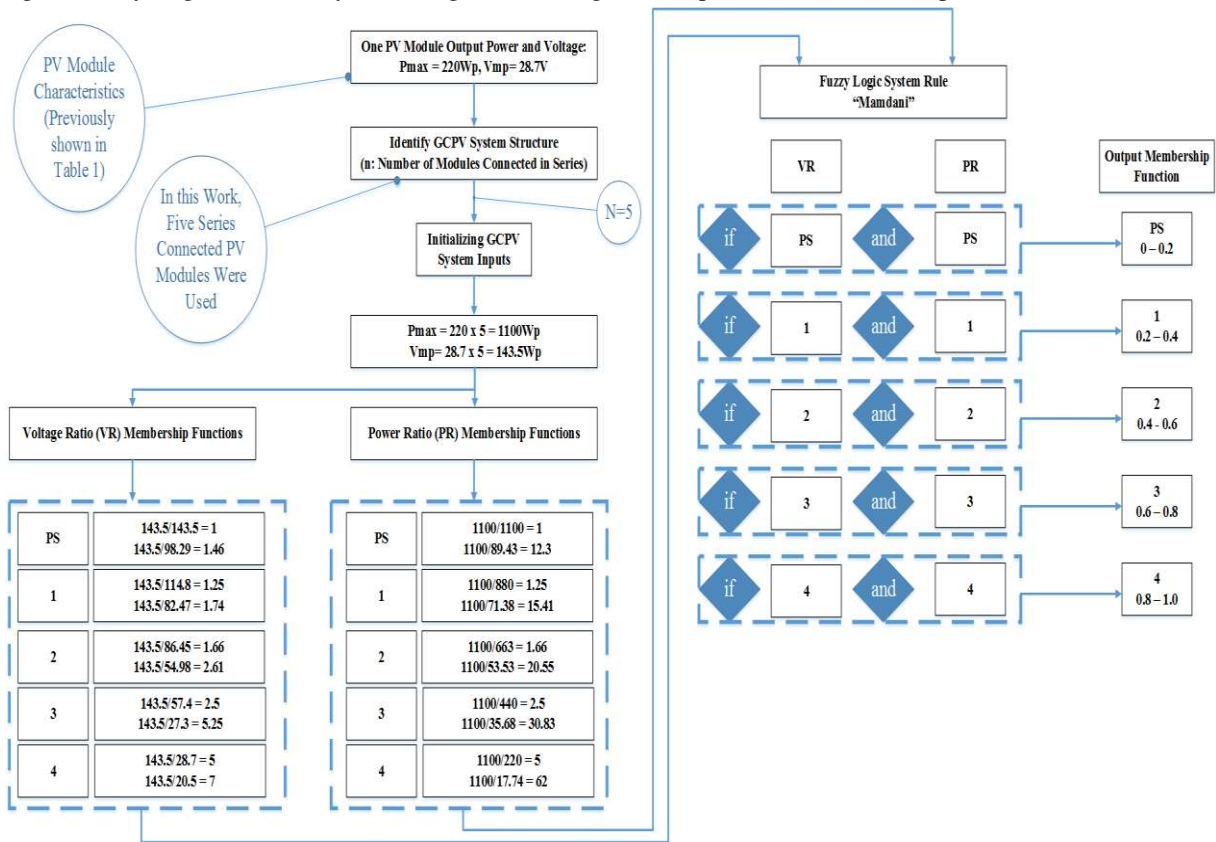


Fig. 5. Mathematical calculations for the fuzzy logic classifier system including VR, PR, Rules and Output Membership Function

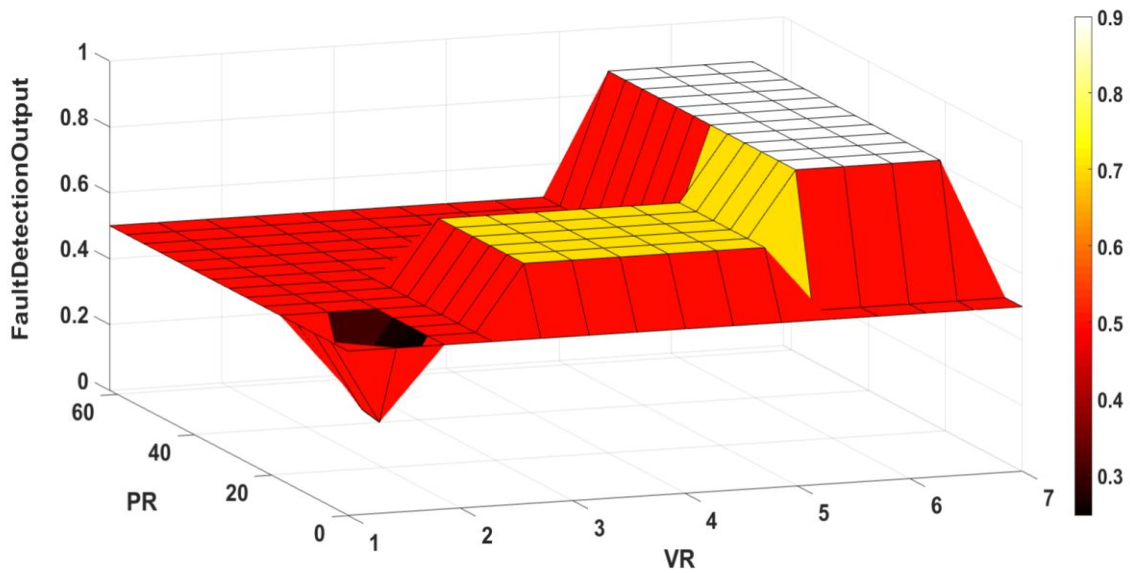


Fig. 6. Fuzzy Logic classifier output surface with VR, PR and the fault detection output membership function

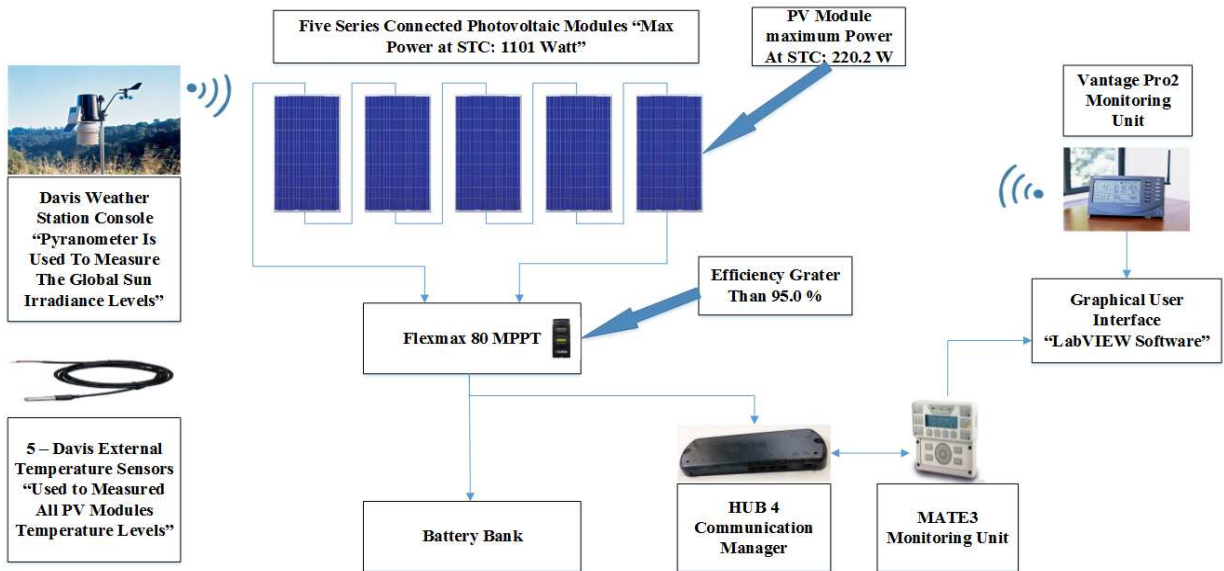


Fig. 7. Examined GCPV Plant Installed at the Huddersfield University, United Kingdom

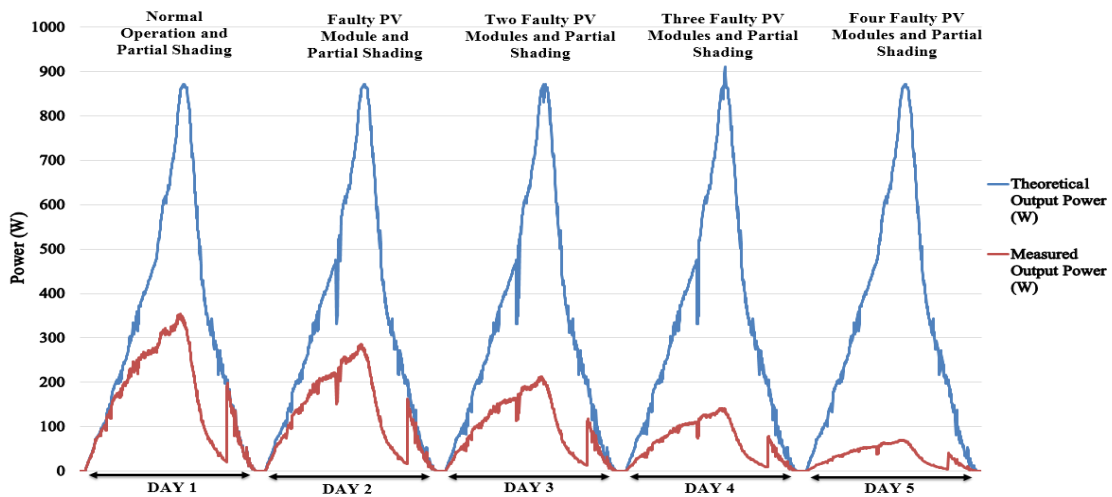


Fig. 8. Theoretical vs. Measured output power during 5 different days

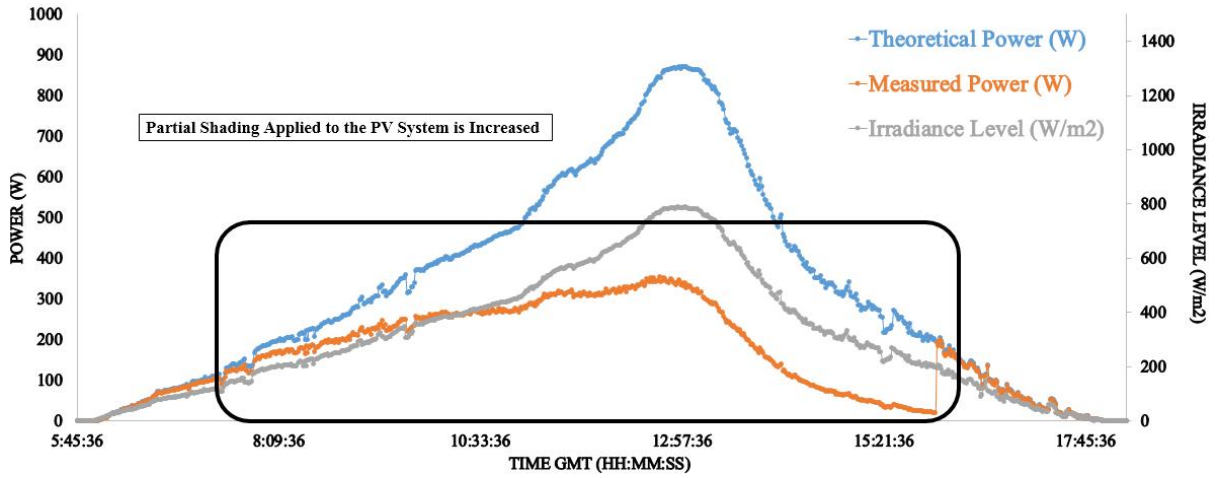


Fig. 9. Theoretical power vs. measured output power for a partial shading effects the GCPV plant

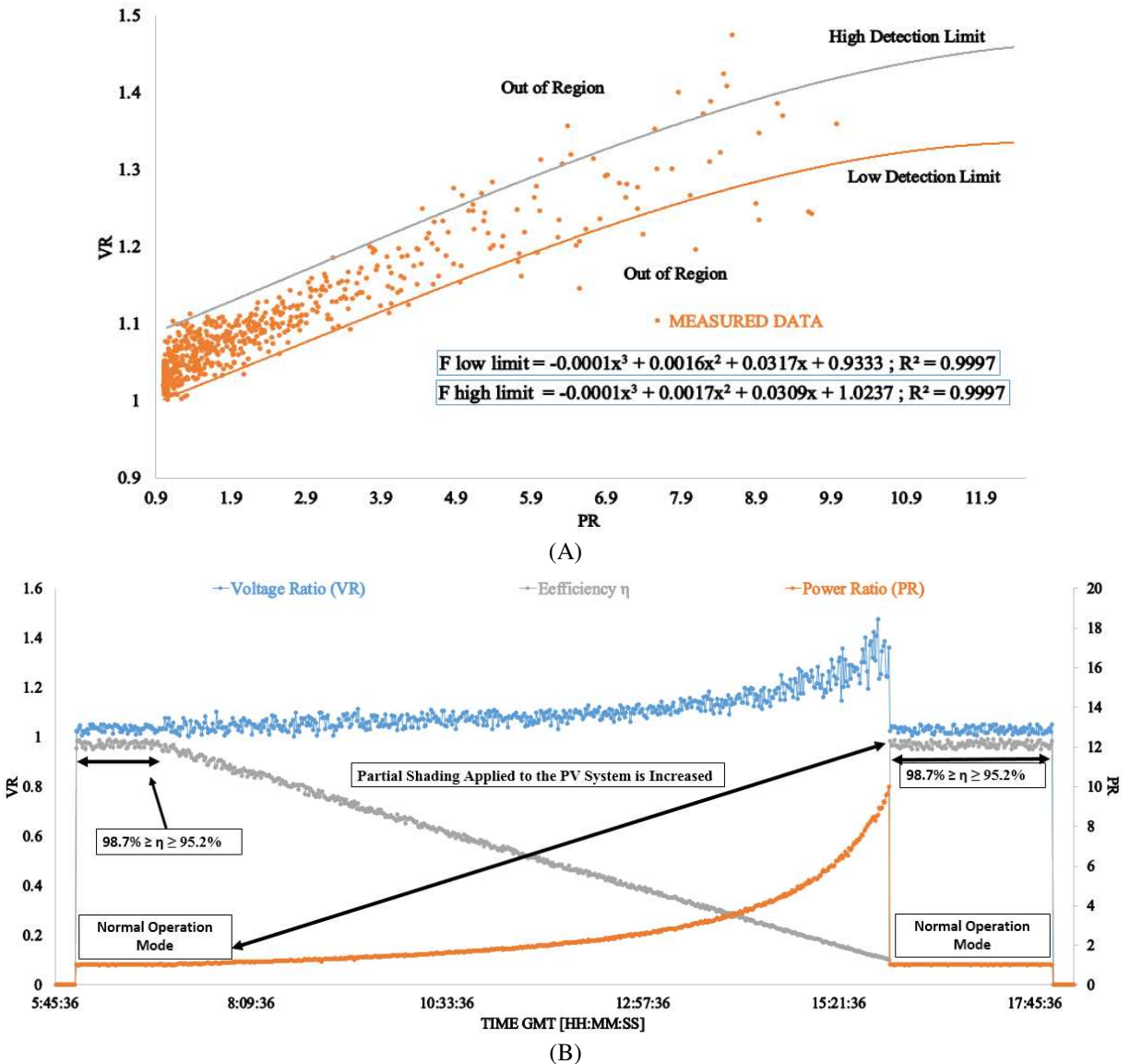


Fig. 10. Theoretical curves vs. real time long term measured data. (A) Theoretical fault curve detection limits for the examined GCPV plant, (B) Voltage ratio, power ratio and the efficiency of the entire GCPV system

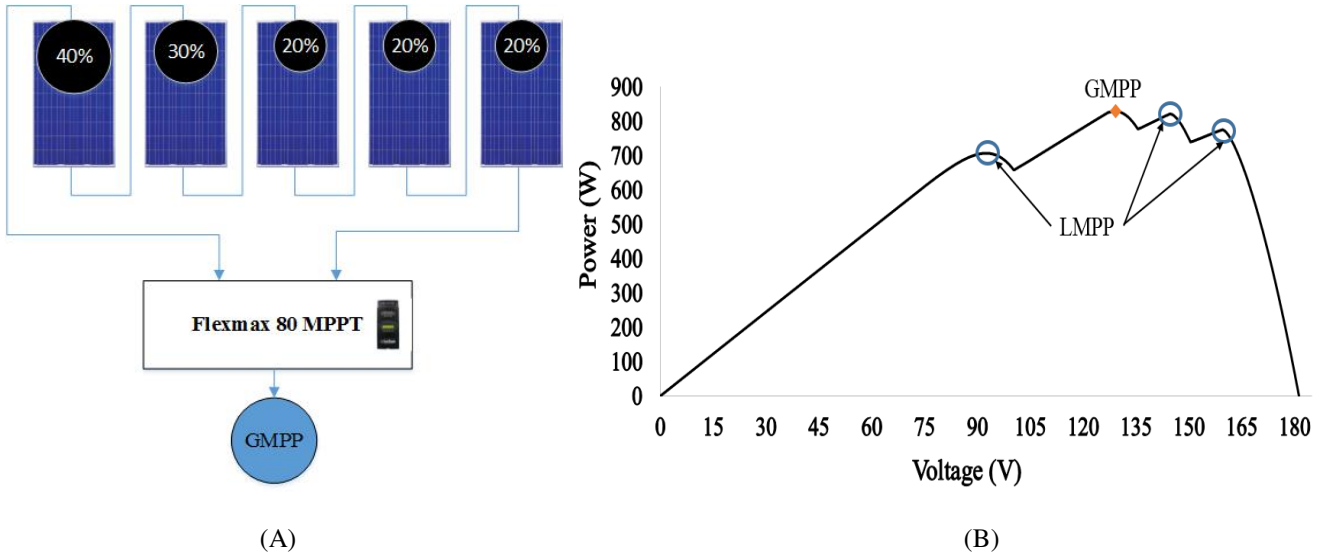


Fig. 11. MPPT unit output power (A) Examined partial shading condition, (B) P-V curve including the output LMPP and GMPP obtained by the MPPT unit

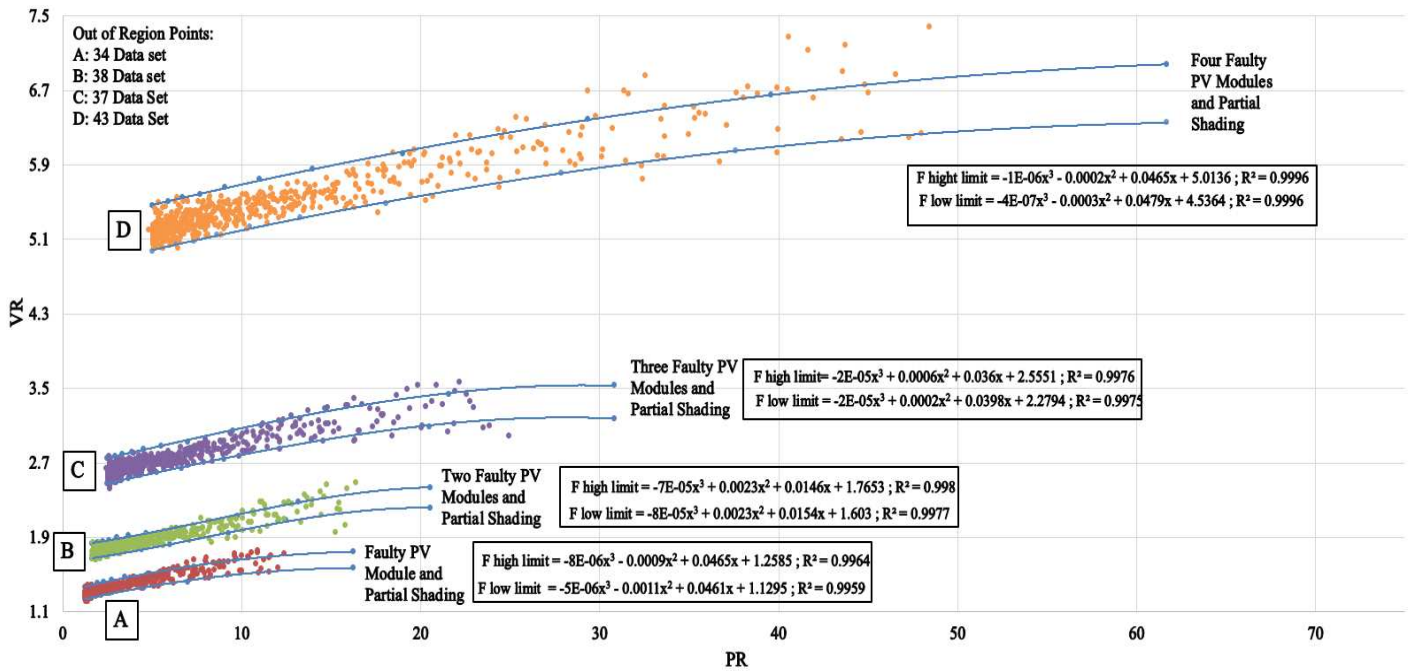


Fig. 12. Theoretical detection limits vs. real-time long-term data measurements for one faulty, two faulty, three faulty and four faulty photovoltaic modules

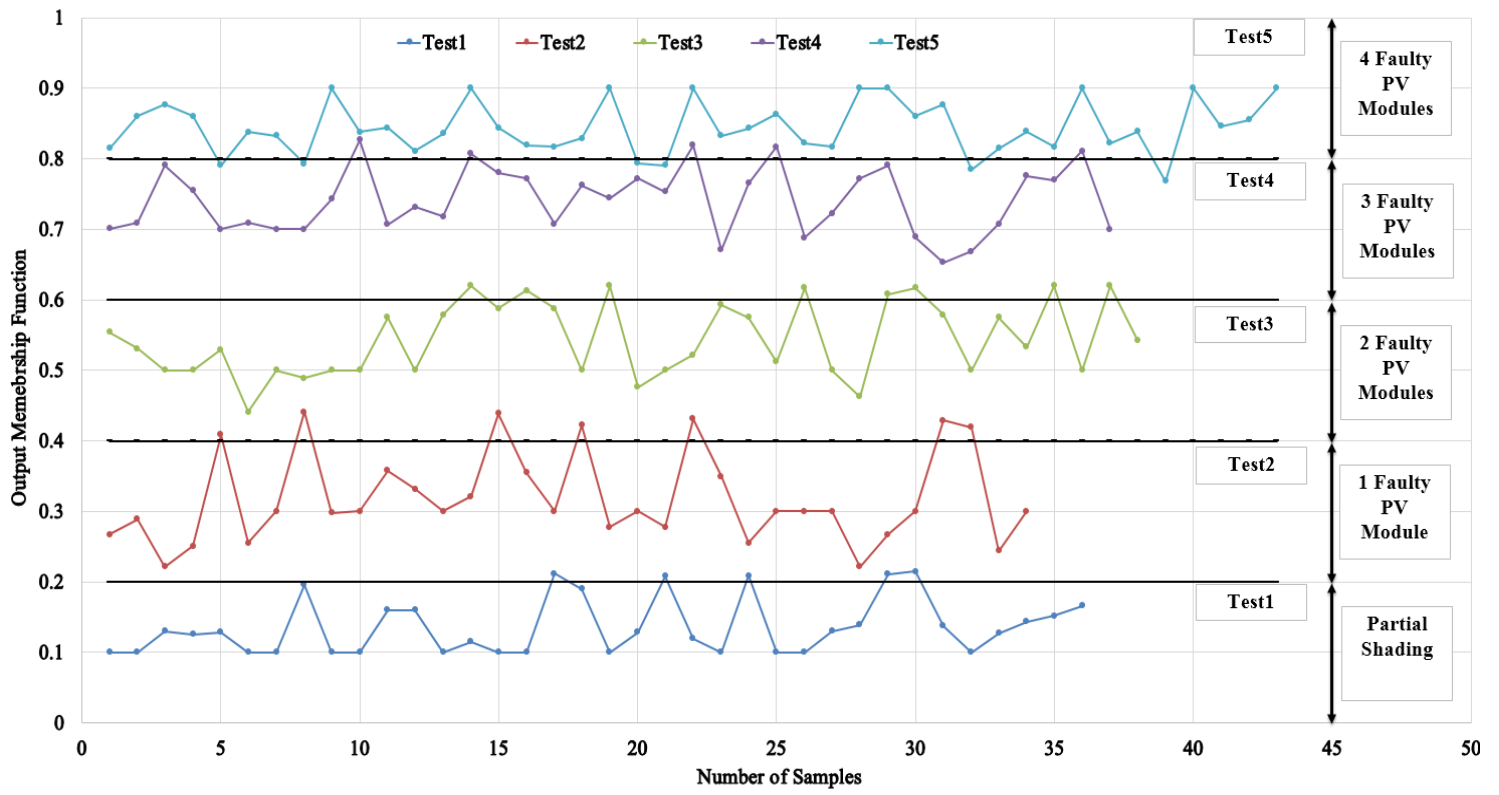
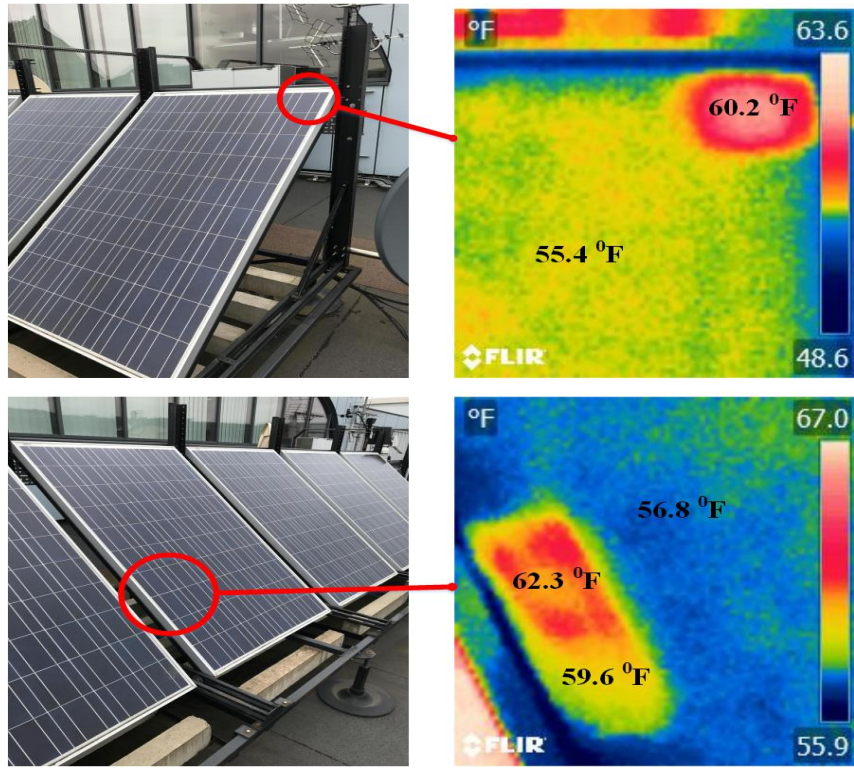
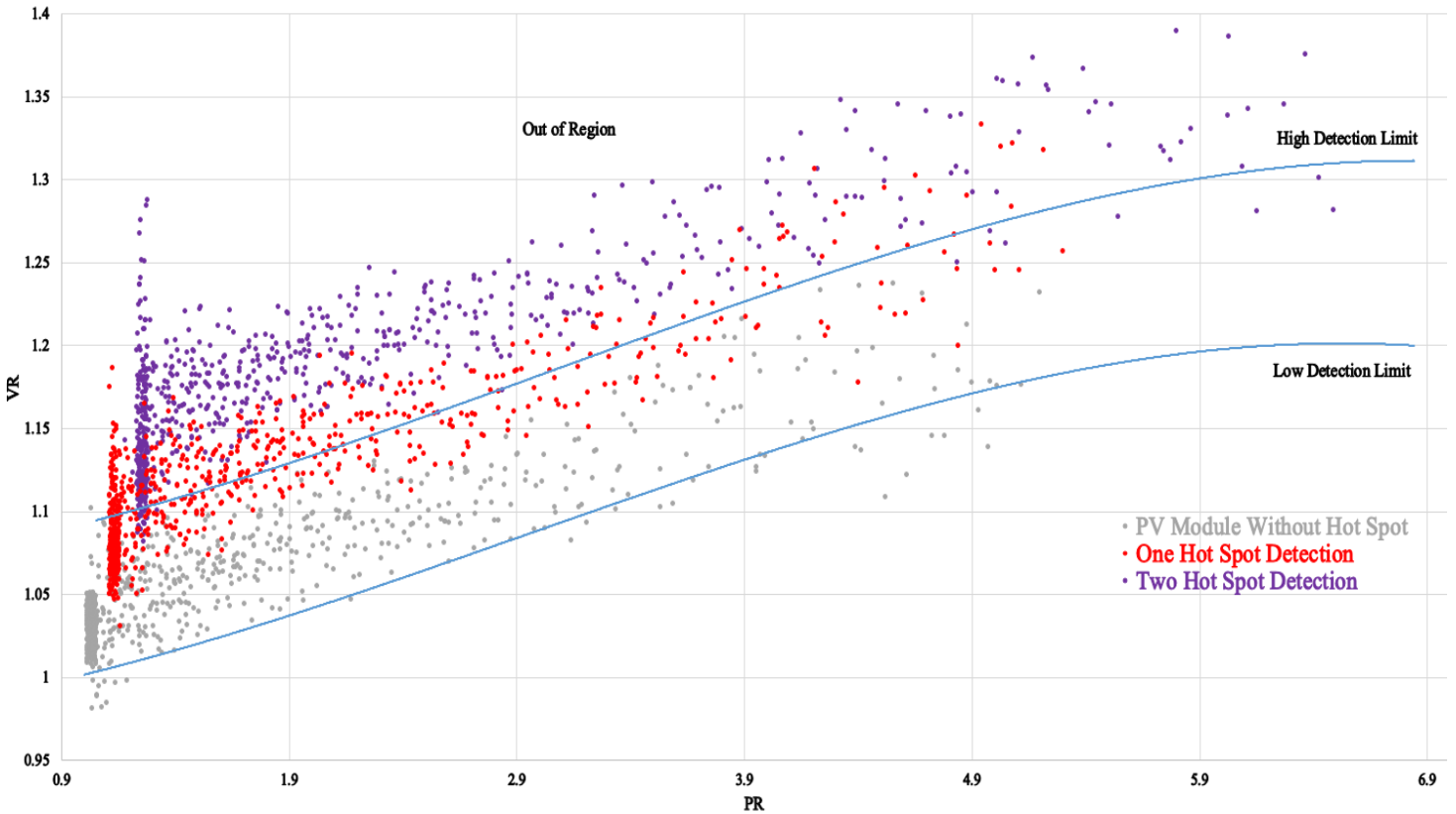


Fig. 13. Out of region samples processed by the fuzzy logic classification system





(A)



(B)

Fig. 14. Theoretical curves vs. real time long term measured data. (A) Hot spot images taken from two different PV modules using FLIR thermal imaging camera, (B) Theoretical fault detection curves vs. measured data obtained from a PV module without hot spots, PV module contains only one hot spot and PV module contains two hot spots

TABLE 1  
Electrical Characteristics of SMT6 (60) P PV Module

Solar Panel Electrical Characteristics	Value
Peak Power	220 W
Voltage at maximum power point ( $V_{mp}$ )	28.7 V
Current at maximum power point ( $I_{mp}$ )	7.67 A
Open Circuit Voltage ( $V_{OC}$ )	36.74 V
Short Circuit Current ( $I_{sc}$ )	8.24 A
Number of cells connected in series	60
Number of cells connected in parallel	1
$R_s$ , $R_{sh}$	0.48 $\Omega$ , 258.7 $\Omega$
dark saturation current ( $I_o$ )	$2.8 \times 10^{-10}$ A
Ideal diode factor (A)	0.9117
Boltzmann's constant (K)	$1.3806 \times 10^{-23}$ J.K <sup>-1</sup>

TABLE 2  
Efficiency Comparison between Four Different Case Scenarios

Test Number	Case Scenario	Without Fuzzy Classifier		Including Fuzzy Classifier	
		Out of Region Samples	Detection Accuracy (DA %)	Out of Region Samples	Detection Accuracy (DA %)
Test 1 (described in section 3.2)	Partial shading effects the GCPV system	37	94.86	5	99.31
Test 2 (presented as A in Fig. 11)	Faulty PV module and partial shading	34	95.27	7	99.03
Test 3 (presented as B in Fig. 11)	Two faulty PV module and partial shading	38	94.72	8	98.80
Test 4 (presented as C in Fig. 11)	Three faulty PV module and partial shading	37	94.86	5	99.31
Test 5 (presented as D in Fig. 11)	Four faulty PV module and partial shading	43	94.03	6	99.16

TABLE 3

Comparative Results between the Proposed Algorithm and the One Presented in Ref. [4], Ref. [7] and Ref. [8]

Case Study		Proposed Algorithm	Ref. [4]	Ref. [8]	Ref. [7]
Year of the Study		2017	2017	2015	2010
Software Used in the Data Analysis		LabVIEW	Not mentioned	Not mentioned	Not mentioned
PV System Capacity		1.1 kWp	1.1 kWp	3.2 kWp	1 <sup>st</sup> : 3 kWp 2 <sup>nd</sup> : 900 Wp
Fault Detection Algorithm Approach	Used Variables	Power and voltage ratios	Voltage and power ratios	Current and voltage ratios	Current and voltage ratios
	Mathematical Modelling	3 <sup>rd</sup> order polynomial function	3 <sup>rd</sup> order polynomial function	Not used	Not used
	Statically Analysis Technique	Using T-test method	Not used	Not used	Not used
	Machine Learning Technique	Mamdani Fuzzy logic	Mamdani Fuzzy logic	Not used	Not used
Type of the Fault Detected	Partial Shading Conditions	√	√	√	√
	Faulty PV Modules	√	√	√	√
	Hot Spots	√	×	×	×